EIGENVALUE ANALYSIS IN ANISOTROPICALLY LOADED ELECTROMAGNETIC CAVITIES USING "EDGE" FINITE ELEMENTS

Jian-She Wang and Nathan Ida

Department of Electrical Engineering
The University of Akron
Akron, OH 44325, U. S. A.

Abstract - The eigenmodes in an arbitrarily shaped, electromagnetic (EM) cavity loaded with an anisotropic material, are computed using linear tetrahedral "edge" elements and curvilinear hexahedral "edge" elements. The permeability tensor is assumed to have off-diagonal entries (gyromagnetic), and the permittivity and conductivity tensors are diagonal (typically for composite materials). Therefore, the divergence free condition is not always satisfied inside a finite element. Yet, the procedure is found to yield good prediction to the lower resonant frequencies, and no spurious modes are encountered in this range of interest. In the examples considered, numerical solutions are consistent with quasi-analytical solutions.

I. INTRODUCTION

The accurate prediction of eigenmodes in inhomogeneously loaded, electromagnetic (EM) cavities is an important subject in the microwave cavity theory and measurement. The use of finite element methods to compute the eigenmodes have been extensively studied in the literature, but spurious solutions are frequently encountered [1,2,3]. Since the spurious solutions have relatively large divergence, the penalty method and the reduction method are commonly used to enforce the divergence free condition, and therefore, eliminate or reduce the nonphysical modes [4,5]. Recent work has shown that, when the "edge" based, divergence free finite elements are used, spurious modes can be deleted [6,7,8]. To the authors' knowledge, the use of "edge" based finite elements to analyze electromagnetic field problems involving anisotropic materials has not been reported. In this paper, we extend the work in [8] to EM cavities loaded with anisotropic materials, which is of significant importance in the microwave cavity nondestructive testing of composite materials. As an example, we compute the eigenmodes in a cylindrical cavity loaded with gyromagnetic or composite materials. This example was considered recently using the Galerkin-Rayleigh-Ritz method [9].

II. FORMULATIONS

The problem under consideration is to find the resonant frequencies and the corresponding field distributions in a dielectric loaded EM cavity. The cavity wall, S, is assumed to be of arbitrary shape. The interior of the cavity, Ω, is characterized by $(\mu_0\overline{\overline{\mu}}_r(\vec{r}), \epsilon_0\overline{\overline{\epsilon}}_r(\vec{r}), \overline{\overline{\sigma}}(\vec{r}))$, where μ_0 and ϵ_0 are free space permeability and permittivity, respectively. Since the cavity contains different materials, $\vec{r}$ is used to denote spatial dependence. The relative permeability, relative permittivity and conductivity are assumed to be the following tensors:

$$\overline{\overline{\mu}}_r = \begin{bmatrix} \mu_{tt} & -j\kappa & 0 \\ j\kappa & \mu_{tt} & 0 \\ 0 & 0 & \mu_{zz} \end{bmatrix}, \quad \overline{\overline{\epsilon}}_r = \begin{bmatrix} \epsilon_{tt} & 0 & 0 \\ 0 & \epsilon_{tt} & 0 \\ 0 & 0 & \epsilon_{zz} \end{bmatrix},$$

$$\overline{\overline{\sigma}} = \begin{bmatrix} \sigma_{tt} & 0 & 0 \\ 0 & \sigma_{tt} & 0 \\ 0 & 0 & \sigma_{zz} \end{bmatrix}. \quad (1)$$

ϵ_{tt} and ϵ_{zz} can have a complex component ϵ''_{tt} and ϵ''_{zz}, respectively. With $e^{j\omega t}$ variation implied, the modes in the cavity must be the solution of one of the following *curlcurl* equations:

$$\nabla \times \overline{\overline{\mu}}_r^{-1}(\vec{r})\nabla \times \vec{E} - k_0^2\overline{\overline{\epsilon}}'_r(\vec{r})\vec{E} = \vec{0}, \quad (2)$$

$$\nabla \times \overline{\overline{\epsilon}}_r'^{-1}(\vec{r})\nabla \times \vec{H} - k_0^2\overline{\overline{\mu}}_r(\vec{r})\vec{H} = \vec{0}, \quad (3)$$

subject to the following divergence free conditions:

$$\nabla \cdot \overline{\overline{\epsilon}}'_r\vec{E} = 0, \qquad \nabla \cdot \overline{\overline{\mu}}_r\vec{H} = 0. \quad (4)$$

The free-space wave number and the complex relative permittivity are given by

$$k_0 = \omega\sqrt{\mu_o\epsilon_0}, \quad \eta_0 = \sqrt{\mu_0/\epsilon_0},$$
$$\epsilon'_{ii} = \epsilon_{ii} - j(\epsilon''_{ii} + \sigma_{ii}\eta_0/k_0), \quad i = t, z. \quad (5)$$

Throughout the paper, k_0 $(rads/m)$ is treated as the resonant frequency for numerical convenience. On material interfaces, $\vec{E}$ and $\vec{H}$ must be tangentially continuous.

To obtain numerical solutions to (2) and (3), it is advantageous to consider their weak forms:

$$\iiint_\Omega \left(\overline{\overline{\mu}}_r^{-1}\nabla \times \vec{E}\right) \cdot (\nabla \times \vec{w}_m)d\Omega - k_0^2\iiint_\Omega \overline{\overline{\epsilon}}'_r\vec{E}\cdot\vec{w}_m d\Omega$$
$$= jk_0\eta_0\iint_S \left(\hat{n}\times\vec{H}\right)\cdot\vec{w}_m dS, \quad (6)$$

$$\iiint_\Omega \left(\overline{\overline{\epsilon}}_r'^{-1}\nabla \times \vec{H}\right) \cdot (\nabla \times \vec{w}_m)d\Omega - k_0^2\iiint_\Omega \overline{\overline{\mu}}_r\vec{H}\cdot\vec{w}_m d\Omega$$
$$= -\frac{jk_0}{\eta_0}\iint_S \left(\hat{n}\times\vec{E}\right)\cdot\vec{w}_m dS, \quad (7)$$

where $\vec{w}_m$ is any set of real vector weighting functions. By virtue of the weak forms, we can define, in the $\vec{E}$ formulation, a homogenous boundary condition $\hat{n}\times\vec{E}$ (an $\vec{H}$ symmetry condition) and a natural boundary condition $\hat{n}\times\vec{H}$ (an $\vec{E}$ anti-symmetry condition). Similarly in the $\vec{H}$ case, $\hat{n}\times\vec{H}$ is the homogenous condition (an $\vec{E}$ symmetry condition), and $\hat{n}\times\vec{E}$ is the natural condition (an $\vec{H}$ anti-symmertry condition). At microwave frequencies, it is quite accurate to assume that the tangential electric field vanishes on the cavity wall. When it is required to take into account the large but finite conductivity in the cavity wall, an impedance boundary condition can be used. This, however, is not considered in this paper. Since (6) and (7) are dual to each other, one needs to solve only one of them. However, they may yield eigenvalue systems of different types, depending on material properties. They also yield eigenvalue systems of different

Manuscript received July 7, 1991

0018-9464/92$03.00

sizes, when boundary and symmetry conditions are imposed. Thus, one may choose $\vec{\mathbf{E}}$ or $\vec{\mathbf{H}}$ as the state variable according to particular problems.

III. "EDGE" FINITE ELEMENTS

To map the eigenproblems into finite dimensions, we use the "edge" based finite element method. There are a number of different "edge" elements reported in the literature. The divergence free hexahedral element of [7] has been found to yield poor results in some cases, and therefore is not used in this work. The tetrahedral element of [10] and the hexahedral element of [11] will be used. The six vector shape functions in a tetrahedron element are

$$\vec{\mathbf{w}}_n(\vec{\mathbf{r}}) = sgn(n)\frac{l_n}{6}\left(\vec{\mathbf{p}}_{7-n,1} \times \vec{\mathbf{p}}_{7-n,2} + \vec{\mathbf{e}}_{7-n} \times \vec{\mathbf{r}}\right), \qquad (8)$$

where $n = 1, 2, \cdots, 6$, and other quantities are defined in [10]. These shape functions are divergence free. If $\bar{\bar{\epsilon}}_r'$ and $\bar{\bar{\mu}}_r$ are diagonal, the divergence free condition (4) will be satisfied inside the element, but may not necessarily so on elemental interfaces. The twelve vector shape functions in a hexahedral element have the form [11]:

$$\vec{\mathbf{w}}_n(\vec{\mathbf{r}}) = \phi_n(\xi, \eta, \zeta)\vec{\mathbf{v}}_n(\vec{\mathbf{r}}), \qquad (9)$$

where $n = 1, 2, \cdots, 12$, ϕ_n are scalar functions defined in the local coordinates. The directional vectors, $\vec{\mathbf{v}}_n$, are modified to allow curvilinear mapping. Apparently, these shape functions are not divergence free. Higher order elements have been constructed, but not used in this work. The following expansions are introduced to approximate the fields in each element:

$$\vec{\mathbf{E}}(\vec{\mathbf{r}}) = \sum_{n=1}^{N} E_n\vec{\mathbf{w}}_n(\vec{\mathbf{r}}), \qquad \vec{\mathbf{H}}(\vec{\mathbf{r}}) = \sum_{n=1}^{N} H_n\vec{\mathbf{w}}_n(\vec{\mathbf{r}}), \qquad (10)$$

where $N = 6$ and 12 for a tetradedral and hexahedral element, respectively, and H_n (or E_n) is the tangential component of $\vec{\mathbf{H}}$ (or $\vec{\mathbf{E}}$) along the n-th edge. Tangential continuities on material interfaces are satisfied. Thus, no special treatment is needed on material interfaces. Each edge has only one unknown, the vector field problem behaves like a scalar problem. In addition, when the tangential components are used as unknowns, the natural boundary condition needs no special care; and the homogeneous boundary condition is forced by setting the corresponding expansion coefficients to zero.. Compared with the conventional finite element procedure, the analysis here is significantly simplified.

IV. DISCRETIZED EIGENVALUE SYSTEMS

With the vector weighting functions chosen to be the same as the shape functions (8) or (9), we obtain various discretised eigensystems. Assume that, on S, $\hat{\mathbf{n}} \times \vec{\mathbf{E}}$ or $\hat{\mathbf{n}} \times \vec{\mathbf{H}}$ are specified. If $\bar{\bar{\mu}}_r$ is not invertible, and especially if $\bar{\bar{\epsilon}}_r'$ does not depend on frequency, the $\vec{\mathbf{H}}$ formulation is preferred. From the weak form (7), we obtain

$$\left([A] - k_0^2[B] + jk_0[G]\right)\ \{H\} \ = \ 0, \qquad (11)$$

where the coefficients of the matrices are given by

$$a_{mn} \ = \ \iiint_\Omega \left(\bar{\bar{\epsilon}}_r'^{-1}\nabla \times \vec{\mathbf{w}}_n\right)\cdot(\nabla \times \vec{\mathbf{w}}_m)d\Omega, \qquad (12)$$

$$b_{mn} \ = \ \iiint_\Omega \bar{\bar{\mu}}_r\vec{\mathbf{w}}_n \cdot \vec{\mathbf{w}}_m d\Omega, \qquad (13)$$

$$g_{mn} \ = \ \frac{1}{\eta_0}\iint_S \hat{\mathbf{n}} \times \vec{\mathbf{E}} \cdot \vec{\mathbf{w}}_m dS. \qquad (14)$$

In other situations, the $\vec{\mathbf{E}}$ formulation is preferred. From the weak form (7), we obtain

$$\left([A] - k_0^2[B] + jk_0([C] + [G])\right)\ \{E\} \ = \ 0, \qquad (15)$$

where the coefficients of the matrices are given by

$$a_{mn} \ = \ \iiint_\Omega \left(\bar{\bar{\mu}}_r^{-1}\nabla \times \vec{\mathbf{w}}_n\right)\cdot(\nabla \times \vec{\mathbf{w}}_m)d\Omega, \qquad (16)$$

$$b_{mn} \ = \ \iiint_\Omega \bar{\bar{\epsilon}}_r(\vec{\mathbf{r}})\vec{\mathbf{w}}_n \cdot \vec{\mathbf{w}}_m d\Omega, \qquad (17)$$

$$c_{mn} \ = \ \iiint_\Omega \eta_0\bar{\bar{\sigma}}(\vec{\mathbf{r}})\vec{\mathbf{w}}_n \cdot \vec{\mathbf{w}}_m d\Omega, \qquad (18)$$

$$g_{mn} \ = \ -\eta_0\iint_S (\hat{\mathbf{n}} \times \vec{\mathbf{H}})\cdot \vec{\mathbf{w}}_m dS. \qquad (19)$$

Equation (15) can be re-arranged into a complex, non-symmetric eigensystem of double size:

$$\begin{bmatrix} A & 0 \\ 0 & B \end{bmatrix}\begin{Bmatrix} E \\ \lambda E \end{Bmatrix} = \lambda\begin{bmatrix} -(C+G) & -B \\ B & 0 \end{bmatrix}\begin{Bmatrix} E \\ \lambda E \end{Bmatrix}. \qquad (20)$$

where $\lambda = jk_0$. If all coefficients are real, (20) is reduced to a real, non-symmetric eigensystem. And finally, when no loss is present, a simple real, symmetric system is obtained:

$$[A]\{E\} = k_0^2[B]\{E\}. \qquad (21)$$

In this work, the QZ algorithm is used to solve complex and real non-symmetric eigensystems, and Lanczos's algorithm is used for real symmetric eigensystems.

V. NUMERICAL EXAMPLES

The procedure discussed above is used next to compute resonant modes in a configuration shown in Fig.1, where a cylindrical cavity contains an anisotropic specimen. This configuration is chosen deliberately because quasi-analytical solutions reported in [9] can be used as a validation of the present procedure.

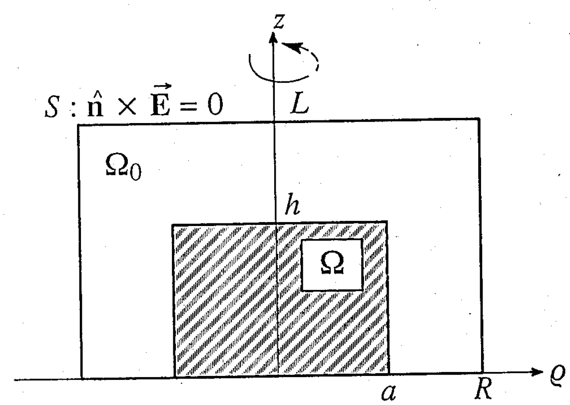

Fig.1 A Cylindrical Anisotropic Specimen in a Cylindrical cavity.

We start with a simpler situation, where the specimen is of the same height as the cavity but different radius, $\mu_{tt} = \mu_{zz} = 1$, $\epsilon_{tt} = 10$, $\sigma_{tt} = \sigma_{zz} = 0$. The problem possesses two way symmetries and has no loss. This allows us to use a relatively larger finite element mesh (794 unknowns per quadrant, not including homogeneous conditions), and the "STLM" code for eigenvalue analysis. The mesh is deliberately designed not to form an "orthogonal mesh". Fig.2 shows the normalized resonant frequencies, $k_0 a\sqrt{\mu_{tt}\epsilon_{tt}}$, versus ϵ_{zz} values. Both tetrahedral and hexahedral models yield roughly the same solution for similar mesh sizes.

If the cavity contains gyromagnetic materials, the permeability tensor has off-diagonal entries. No symmetry planes can be used here. Although the medium is lossless, it is necessary to operate in the complex domain. Fig.3 shows the normalized resonant frequencies of seven lower modes versus $|\kappa/\mu|$ values, when the cavity is completely filled with a gyromagnetic material. Fig.4 shows the normalized resonant frequencies of four lower modes versus $|\kappa/\mu|$ values, when the cavity is partially loaded with a gyromagnetic specimen.

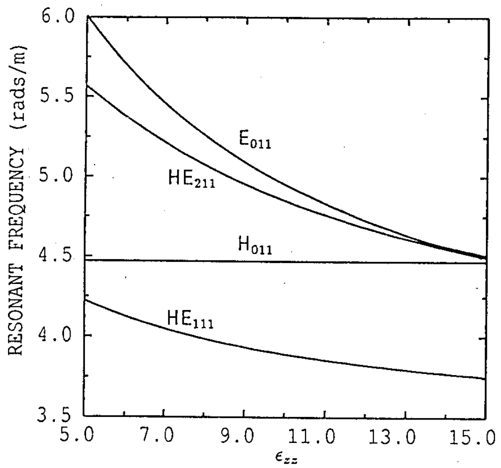

Fig.2 Normalized Resonant Frequencies versus ϵ_{zz} values, when $L = h = a$, $R = 2a$, $\epsilon_{tt} = 10$, $\sigma_{tt} = \sigma_{zz} = 0$, $\mu_{tt} = \mu_{zz} = 1$, $\kappa = 0$.

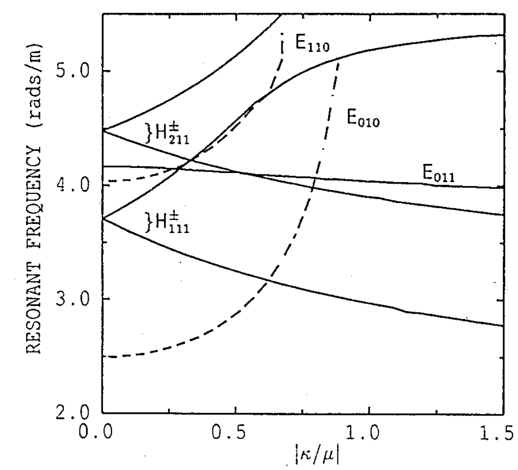

Fig.3 Normalized Resonant Frequencies versus $|\kappa/\mu|$ values, when $L = h = a$, $R = 2a$, $\epsilon_{tt} = 10$, $\sigma_{tt} = \sigma_{zz} = 0$, $\mu_{tt} = \mu_{zz} = 1$.

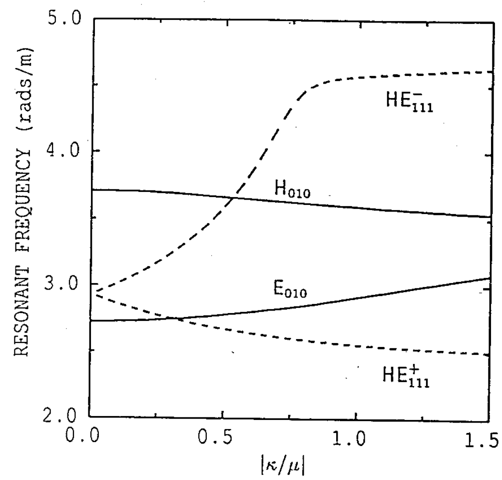

Fig.4 Normalized Resonant Frequencies versus $|\kappa/\mu|$ values, when $h = a$, $L = R = 2a$, $\epsilon_{tt} = \epsilon_{zz} = 10$, $\sigma_{tt} = \sigma_{zz} = 0$, $\mu_{tt} = \mu_{zz}$.

The mode patterns shown in Fig.2 to Fig.4 are consistent with the Rayleigh-Ritz-Galerkin solutions of [9].

The procedure is also used to analyze lossy problems. Two situations are given. Fig.5 shows the normalized resonant frequencies of four modes when ϵ''_{zz} is varied. Fig.6 shows the normalized resonant frequencies of four modes when σ_{zz} is varied. Although no available data can be used for validation, the mode patterns obviously resemble those shown in Fig.2.

Although the geometry shown in Fig.1 has a rotational symmetry, our procedure, however, is not limited to this configuration.

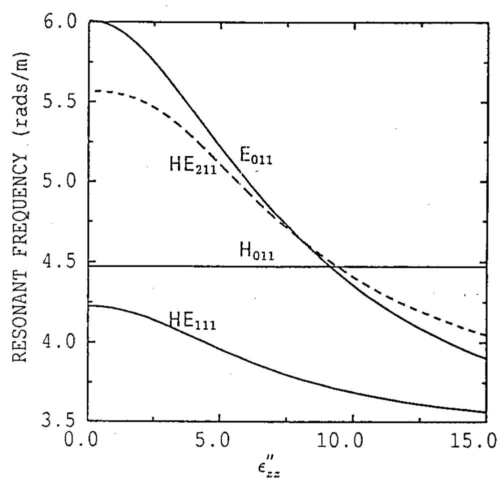

Fig.5 Normalized Resonant Frequencies versus ϵ''_{zz} values, when $L = h = a$, $R = 2a$, $\epsilon_{tt} = 10$, $\epsilon_{zz} = 5$, $\sigma_{tt} = \sigma_{zz} = 0$, $\mu_{tt} = \mu_{zz} = 1$, $\kappa = 0$.

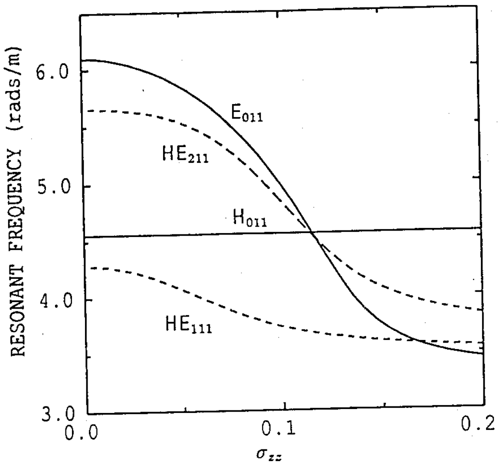

Fig.6 Normalized Resonant Frequencies versus σ_{zz} values, when $L = h = a$, $R = 2a$, $\epsilon_{tt} = 10$, $\epsilon_{zz} = 5$, $\sigma_{tt} = 0$, $\kappa = 0$, $\mu_{tt} = \mu_{zz} = 1$.

VI. CONCLUSIONS

Linear tetrahedral "edge" elements and curvilinear hexahedral "edge" elements were used to compute the eigenmodes in EM cavities loaded with anisotropic materials (gyromagnetic and composite, in particular). In spite of the fact that the divergence free condition was not always satisfied inside a finite element, our procedure gave good prediction to the lower resonant frequencies, as validated against quasi-analytical solutions. No spurious modes occurred in the lower range of frequencies. While our study showed the importance of maintaining tangential continuities of $\vec{E}$ and $\vec{H}$ in vector field computation, it remains a future task to find theoretical explainations why non-divergence free "edge" elements yield no spurious solutions, and to examine more complicated situations.

ACKNOWLEDGMENT

This work was supported in part by NSF Grant #EET8714628 and in part by The Ohio Board of Regents Academic Challenge Program. Computational Resources on the Ohio Supercomputer Center CRAY Y-MP are gratefully acknowledged. The "STLM" code used to solve real symmetric eigenvalue problems was provided by Thomas Ericsson, Department of Computer Science, Chalmers University of Technology, Sweden. Special thanks go to Dr. A. Bossavit for calling the authors' attention to the fact that, divergence free "edge" elements may not be divergence free on elemental interfaces.

REFERENCES

[1] J. B. Davies, F. A. Fernandez and G. Y. Philippou, "Finite Element Analysis of All Modes in Cavities with Circular Symmetry", IEEE Trans. Microwave Theory and Techniques, Vol. MTT-30, No.11, pp. 1975 - 1980, 1982.

[2] M. Hara, T. Wada, T. Fukusawa and F. Kikuchi, "A Three Dimensional Analysis of RF Electromagnetic Fields by the Finite Element Method", IEEE Trans. Magnetics, Vol. MAG-19, No.6, pp. 2417 - 2420, 1983.

[3] J. P. Webb, "The Finite-Element Method for Finding Modes of Dielectric-Loaded Cavities", IEEE Trans. Microwave Theory and Techniques, Vol. MTT-33, No.7, pp. 635 - 639, 1985.

[4] J. P. Webb, "Efficient Generation of Divergence - Free Fields for the Finite Element Analysis of 3D Cavity Resonators", IEEE Trans. Magnetics, Vol. MAG-24, No.1, pp. 162 - 165, 1988.

[5] A. Konrad, "A Method for Rendering 3D Finite Element Vector Field Solutions Non-Divergent", IEEE Trans. Magnetics, Vol. MAG-25, No.4, pp. 2822 - 2824, 1989.

[6] A. Bossavit, "Solving Maxwell Equations in a Closed Cavity, and The Question of 'Spurious Modes'", IEEE Trans. Magnetics, Vol.26, No.2, 1990, pp. 702 - 705.

[7] K. Sakiyama, H. Kotera and A. Ahagon, "3-D Electromagnetic Field Mode Analysis Using Finite element Method by Edge Element", IEEE Trans. Magnetics, Vol.26, No.5, pp. 1759 - 1761, 1990.

[8] Jian-She Wang, Nathan Ida: "Eigenvalue Analysis in EM Cavities Using Divergence Free Finite Elements", EFC 1990.

[9] J. Krupka, "Resonant Modes in Shielded Cylindrical Ferrite and Single-Crystal Dielectric Resonantors", IEEE Trans. Microwave Theory and Techniques, Vol.37, No.4, pp. 691 - 697, 1989.

[10] M. L. Barton and Z. J. Cendes, "New Vector Finite Elements for Three-Dimensional Magnetic Field Computation", J. Appl. Phys., Vol.61, No.8, 1987, pp. 3919 - 3921.

[11] J. S. van Welij, "Calculation of Eddy Currents in terms of H on Hexahedra", IEEE Trans. Magnetics, Vol.MAG-21, No.6, pp. 2239 - 2241, 1985.